Effect of nucleon exchange on projectile multifragmentation in the reactions of ^{28}Si+^{112}Sn and ^{124}Sn at 30 and 50 MeV/nucleon

M. Veselsky,* R. W. Ibbotson,† R. Laforest,‡ E. Ramakrishnan,§ D. J. Rowland, A. Ruangma, E. M. Winchester, E. Martin, and S. J. Yennello

Cyclotron Institute, Texas A&M University, College Station, Texas 77843

(Received 9 February 2000; published 15 November 2000)

The multifragmentation of quasiprojectiles was studied in the reactions of a ^{28}Si beam with ^{112}Sn and ^{124}Sn targets at projectile energies of 30 and 50 MeV/nucleon. The quasiprojectile observables were reconstructed using isotopically identified charged particles with $Z_f \leqslant 5$ detected at forward angles. The nucleon exchange between projectile and target was investigated using the isospin and the excitation energy of the reconstructed quasiprojectile. For events with total reconstructed charge equal to the charge of the beam ($Z_{tot}=14$), the influence of the beam energy and target isospin on the neutron transfer was studied in detail. Simulations were carried out employing a model of deep inelastic transfer, a statistical model of multifragmentation, and a software replica of the FAUST detector array. The concept of deep inelastic transfer provides a good description of the production of highly excited quasiprojectiles. The isospin and excitation energy of the quasiprojectile were described with good overall agreement. The fragment multiplicity, charge and isospin were reproduced satisfactorily. The range of contributing impact parameters was determined using a backtracing procedure.

PACS number(s): 25.70.Mn, 25.70.Pq

INTRODUCTION

Projectile fragmentation has traditionally been thought of as a two-step reaction with excitation via a peripheral collision with the target followed by fragmentation of the projectile. In this framework, the influence of the mass and charge of the target nucleus on projectile fragmentation is a question of interest both with regard to the formation of the excited quasiprojectile and its subsequent fragmentation. The target nucleus may affect fragmentation of the projectile in various ways. Charity *et al.* report the influence of the repulsive Coulomb field of the target on the motion of the emitted charged particles [1]. The influence of isospin equilibration on reaction dynamics has been studied at lower energies [2–4]. De Souza *et al.* [2] showed that the nucleon exchange is regulated by the potential energy surface if isospin equilibration is allowed to occur. At low energies below 10 MeV/nucleon, the studies of nucleon transfer [3,4] showed deviations from the predictions of the commonly used model of nucleon exchange [5] in the description of a proton and neutron drift. At intermediate energies up to 50 MeV/nucleon, the model of nucleon exchange successfully describes the production of the projectilelike nuclei at forward angles [6]. The influence of isospin on the cooling of the interacting system by emission of fast nucleons was observed in the study of multifragmentation of the systems ^{112}Sn+^{112}Sn and ^{124}Sn+^{124}Sn at a broad range of impact parameters [7].

In the current study we present a continuation of our previous work on projectile multifragmentation of a ^{28}Si beam in the reaction with ^{112}Sn and ^{124}Sn targets at 30 and 50 MeV/nucleon [8]. We select the events consisting of isotopically identified fragments in order to reconstruct the mass and charge of the fragmenting projectilelike nucleus. The N/Z difference of the Sn isotopes used as targets is significant enough to permit the study of the influence of neutron excess on production and deexcitation of the projectilelike nucleus. The study is divided into several sections. We present a short description of the experimental setup, a discussion of the nucleon exchange (dissipation) mechanism, divided into an analysis of the experimental observables of the reconstructed quasiprojectile and a comparison to the results of simulations, and a discussion of multifragmentation of excited quasiprojectiles. Finally a short summary will be presented.

EXPERIMENT

The experiment was done with a beam of ^{28}Si impinging on $\sim$1 mg/cm^2 self-supporting ^{112,124}Sn targets. The beam was delivered at 30 and 50 MeV/nucleon by the K500 superconducting cyclotron at the Cyclotron Institute of Texas A&M University. The detector array FAUST [9] consisted of 68 silicon-CsI(Tl) telescopes covering polar angles from 2.3° to 33.6° in the laboratory system. Each element is composed of a 300 μm surface barrier silicon detector followed by a 3 cm CsI(Tl) crystal. The detectors are arranged in five concentric rings. The geometrical efficiency is approximately 90% for the angle range covered. These detectors allow isotopic identification of light charged particles and intermediate-mass fragments up to a charge of $Z_f=5$. The

*Electronic address: veselsky@comp.tamu.edu. On leave of absence from Institute of Physics of SASc, Bratislava, Slovakia.

†Present address: Brookhaven National Laboratory, Brookhaven, NY 11973.

‡Present address: Mallinckrodt Institute of Radiology, St. Louis, MO 63110.

§Present address: Microcal Software Inc., One Roundhouse Plaza, Northampton, MA 01060.

energy thresholds are determined by the energy needed to punch through the 300 μm silicon detector. These energy thresholds have little effect on the acceptance of particles from the fragmenting projectile due to the boost from the beam energy. Details of the experimental procedure and detector calibration can be found in Ref. [8]. Additional silicon telescopes complemented the forward array in the setup. A telescope consisting of a 53 μm silicon detector, 147 μm silicon strip detector (16 strips), and a 994 μm silicon detector was placed at 40° in the laboratory. The 53 and 994 μm silicons had an active area of 5 cm$\times$5 cm and were divided in four quadrants. This telescope covered the polar angle from 42.5° to 82.2°. Another silicon telescope was placed at 135° in the lab, covering polar angles from 123° to 147°. It was composed of two 5 cm$\times$5 cm active area silicon detectors of thickness 135 and 993 μm, respectively. A 2 cm thick CsI(Tl) detector read out via a photodiode was placed behind both silicon pairs.

In the present study we restrict ourselves to the events where all emitted fragments are isotopically identified ($Z_f < 5$). We assume that such events detected in the FAUST detector array originate predominantly from the deexcitation of the quasiprojectile (or projectilelike source). The total charge of the reconstructed quasiprojectile (QP) is restricted to the values near the projectile charge ($Z_{\rm tot}=12-15$). This very selective data contains information on fragmentation of highly excited projectilelike prefragments, and thus can be used for the study of the mechanism of dissipation of the kinetic energy of relative motion into thermal degrees of freedom. The high granularity of FAUST, the moderate beam current, and the high selectivity of the events allowed us to minimize the number of pile-up signals.

NUCLEON EXCHANGE

Nucleon exchange is supposed to be a highly effective mechanism of dissipation of the kinetic energy of relative motion of the projectile and target into their internal degrees of freedom. In this section we present an overview of experimental observables of the reconstructed quasiprojectile and a comparison to the results of simulations.

Experimental observables

In order to identify an emitting source from which the detected fragments originate, we reconstructed the velocity distributions of the quasiprojectiles with total charge $Z_{\rm tot}=12-15$ for the set of events where all emitted fragments are isotopically identified. Resulting velocity distributions for projectile energies 30 and 50 MeV/nucleon are given in Figs. 1(a) and 1(b). Solid squares represent the reaction with ^{112}Sn target and open squares reaction with ^{124}Sn. For a given projectile energy, the mean velocities and widths of distributions are practically identical for both targets. The velocity distributions are close to Gaussians over two orders of magnitude (Gaussian fits are given as solid lines). The observed velocity distributions are symmetric and have no significant low- or high-energy tails. Thus, the reconstructed quasiprojectiles may indeed be identified with the projectilelike

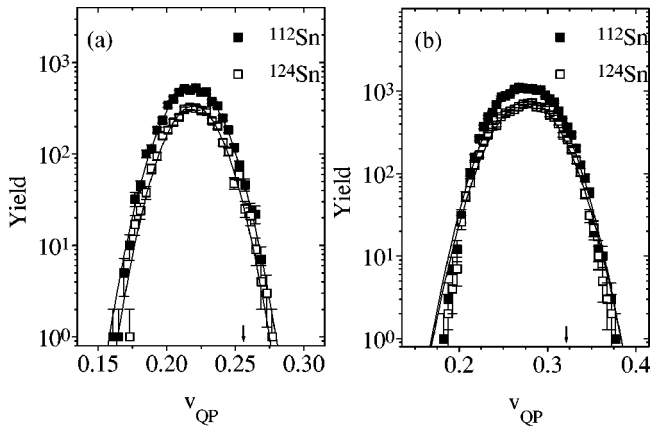

FIG. 1. Experimental velocity distributions of the fully isotopically resolved quasiprojectiles with $Z_{\rm tot}=12-15$ [solid and open squares mean ^{112}Sn and ^{124}Sn target, (a) and (b) the projectile energy 30 and 50 MeV/nucleon, respectively]. Solid lines show Gaussian fits.

fragment source. The admixture of particles from the midvelocity sources such as preequilibrium or neck emission, if any, does not distort the Gaussian shape of the quasiprojectile velocity distributions. The mean velocities of the sources are somewhat lower than the velocity of the beam (indicated by arrows), which indicates the damping of the kinetic energy into internal degrees of freedom.

Useful experimental information about the nucleon exchange rate can be found in the events where the charge of the reconstructed quasiprojectile is equal to the charge of incident beam ($Z_{\rm tot}=14$). In this case, isospin equilibration may only occur by the transfer of neutrons, as the number of transferred neutrons is the only available isospin degree of freedom of the system. Since the neutron number of the reconstructed quasiprojectile is just the sum of neutrons bound in the fragments with nonzero charge, we define the principal neutron exchange observable as the mass change. Subtracting the sum of the neutrons bound in detected fragments from the neutron number of the beam gives

$$\Delta A = N_{\rm proj} - \sum_f N_f, \tag{1}$$

where $N_{\rm proj}=14$ for ^{28}Si beam. A positive value of this observable means that the neutron number of the reconstructed quasiprojectile is lower than the neutron number of the projectile and one or more projectile neutrons have been lost by transfer to the target nucleus and/or by emission in the fragmentation stage. A positive value of ΔA may also be obtained in a collision where the transfer of one or more neutrons from the target to the projectile occurs but a larger number of neutrons is emitted later. Finally, a negative value of ΔA means that the neutron flow from target to projectile is stronger than emission.

The resulting mass change distributions for both projectile energies and target isotopes are shown in Fig. 2 (^{112}Sn: solid circles, ^{124}Sn: open circles). The mass change depends on the target nucleus and beam energy. For both projectile energies the mean value of the mass change is larger for the

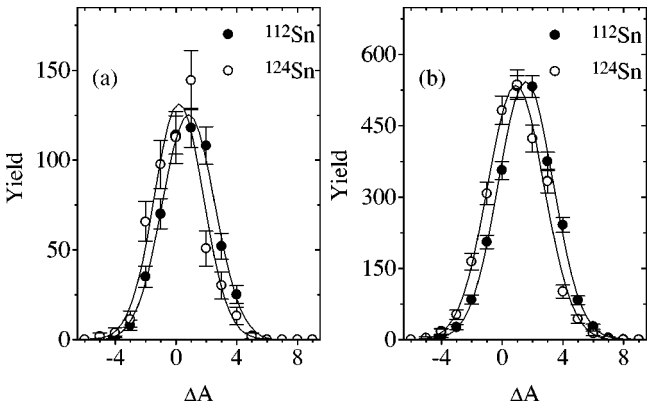

FIG. 2. Experimental distributions of the mass change for fully isotopically resolved quasiprojectiles with $Z_{tot}=14$ [solid and open circles mean ^{112}Sn and ^{124}Sn target, (a) and (b) the projectile energy 30 and 50 MeV/nucleon, respectively]. Solid lines show Gaussian fits.

reaction with the ^{112}Sn target by a little more than half a unit (0.60 for 30 MeV/nucleon and 0.65 for 50 MeV/nucleon, see Table I). Therefore, there could be more neutrons transferred from the target to the projectile during the interaction with ^{124}Sn target, or there could be more neutrons emitted from the quasiprojectile that interacted with the ^{112}Sn target, or more neutrons could be transferred from the projectile to the ^{112}Sn target. The relative importance of different processes may be deduced from the sign of the mean values of the ΔA distributions. As one can see in Table I, they are positive in all cases. For the events with $Z_{tot}=14$, where the proton degree of freedom is fixed, the only possible way to achieve isospin equilibrium of the interacting dinuclear system is with neutron flow from the target to the projectile. Thus, especially in the case of neutron rich ^{124}Sn target, the positive values of $\langle \Delta A \rangle$ provide evidence for the influence of the neutron emission on the final neutron content of the quasiprojectile. Indeed, when comparing the mean values of the mass change for the reactions with the same target nucleus at different projectile energies, the mean mass change significantly increases with an increase of beam energy from 30 to 50 MeV/nucleon (0.73 for ^{112}Sn and 0.68 for ^{124}Sn).

When looking at the shapes of the observed ΔA distributions, it is apparent that they are almost identical for different targets at the same projectile energy and are close to ideal Gaussians. The relative shift between systems is given by the mean values discussed above. The width of the ΔA distributions increases slightly (see Table I) with increasing projectile energy. The Gaussian shapes of the ΔA distributions may be understood as an additional argument for the presence of the nucleon exchange in the early stage of the reaction because they resemble the predictions of the theory of deep inelastic transfer (DIT) [5,10,11]. Within this theoretical concept, Gaussian shapes of the mass and charge distributions are obtained as solutions of transport equations (e.g., Fokker-Planck) for the mass and charge degrees of freedom. Thus, the experimental mean values and shapes of the mass change distributions suggest the general picture where the mass change is a combination of the number of neutrons transferred between projectile and target during the interaction phase of the reaction and of the number of neutrons emitted from the excited quasiprojectile.

The apparent charged particle excitation energy of the quasiprojectile can be reconstructed for each projectile fragmentation event from the energy balance in the center-of-mass frame of the quasiprojectile. Thus

$$E^*_{app}=\sum_f (T_f^{QP}+\Delta m_f)-\Delta m_{QP}, \qquad (2)$$

where T_f^{QP} is the kinetic energy of the fragment in the reference frame of the quasiprojectile and Δm_f and Δm_{QP} are the mass excesses of the fragment and quasiprojectile, respectively. Emitted neutrons are not included in this observable, but for these light fragmenting systems neutron emission is not expected to dominate. Therefore, E^*_{app} can provide a relative comparison of the excitation energy of the fragmenting source at the end of the dynamic evolution of the projectile-target system. The distributions of the apparent quasiprojectile excitation energies reconstructed from fully isotopically resolved events are shown in Fig. 3. The reconstructed distributions for the multifragmentation events with $Z_{tot}=14$ are represented as circles (^{112}Sn: solid circles, ^{124}Sn: open circles). The squares represent the broader set of events with $Z_{tot}=12-15$ (^{112}Sn: solid squares, ^{124}Sn: open squares). Mean values of the apparent quasiprojectile excitation energies do not significantly differ for different targets at the same projectile energy and increase with increasing projectile energy (see Table I). Similar mean values of the excitation energy of reconstructed quasiprojectiles for different tar-

TABLE I. Mean values and widths of experimental distributions of the mass change (ΔA) and of the apparent quasiprojectile excitation energy (E^*_{app}) for the fully isotopically resolved quasiprojectiles.

			$Z_{tot}=14$			$Z_{tot}=12-15$	
E_{proj} (MeV/nucleon)	Target	$\langle \Delta A \rangle$	$\sigma_{\langle \Delta A \rangle}$	$\langle E^*_{app} \rangle$ (MeV)	$\sigma_{\langle E^*_{app} \rangle}$ (MeV)	$\langle E^*_{app} \rangle$ (MeV)	$\sigma_{\langle E^*_{app} \rangle}$ (MeV)
30	^{112}Sn	0.81	1.63	101.2	25.8	114.9	25.0
	^{124}Sn	0.21	1.63	102.3	27.0	120.2	28.3
50	^{112}Sn	1.54	1.82	142.8	37.9	160.8	36.7
	^{124}Sn	0.89	1.82	142.8	38.1	161.2	38.1

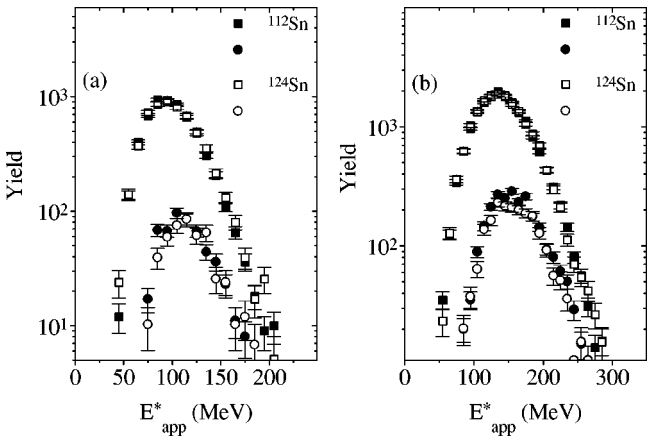

FIG. 3. Experimental distributions of the reconstructed apparent excitation energy of the quasiprojectiles [circles: $Z_{tot}=14$, squares: $Z_{tot}=12-15$, solid and open symbols: ^{112}Sn and ^{124}Sn target, (a) and (b): projectile energy 30 and 50 MeV/nucleon].

gets at the same projectile energy suggest similar time evolution of the dissipating system.

The shapes of the excitation energy distributions exhibit a strong threshold behavior at low energy and a fast decrease in the high energy part which makes them quite narrow. They are slightly asymmetric with an excess of yield at high energy. The thresholdlike behavior may be explained by the existence of energy thresholds for the deexcitation channels with emission of fragments with $Z_f \leqslant 5$. Indeed, the low-energy threshold behavior does not dramatically change with increasing projectile energy. On the other hand, the high-energy part may be influenced by various factors. The production cross section decreases with increasing excitation energy of the quasiprojectile. However, it may also be influenced by the decrease of the detection efficiency of FAUST for multifragmentation events with high multiplicity and large transverse momentum. When comparing the shapes of excitation energy distributions at different projectile energies, the low-energy part is comparable at both projectile energies and the range of the excitation energies to which the high-energy part extends increases with projectile energy, thereby increasing the widths of quasiprojectile excitation energy distributions.

In order to estimate the influence of target multifragmentation on the multiplicity of charged particles, detected at forward angles, we used several telescopes positioned at central and backward angles for detection of charged particles emitted in coincidence with the quasiprojectiles with total charge $Z_{tot}=12-15$ where all emitted fragments are isotopically identified. Only light charged particles ($Z \leqslant 2$) were detected at angles between 42.5° and 147°. The measured yields of light charged particles were low (typically several tens or a few hundreds of particles per detector) what means the rate not exceeding 0.1 particle detected per isotopically resolved quasiprojectile with total charge $Z_{tot}=12-15$. The yields of charged particles are approximately two times higher for the target nucleus ^{112}Sn than for ^{124}Sn, which may be explained by the lower N/Z ratio of ^{112}Sn. The low multiplicity of coincident charged particles implies that the deexcitation of quasitarget is dominated by the emission of neutrons, which are not detected in our experiment. Although the measured spectra could not be used to estimate the slope temperature, we made a rough estimate of the temperature of quasitarget from the mean kinetic energy. For an ideal Maxwellian spectra, the mean kinetic energy of emitted particles above corresponding Coulomb barrier is twice the temperature. Assuming ideal Maxwellian shape of the measured spectra of protons, the values of temperature ranged from 3 to 3.5 MeV for both targets and projectile energies.

Simulations

Experimental distributions of the quasiprojectile observables presented above suggest an interplay of nucleon exchange in the early stage, leading to partial isospin equilibrium, followed by emission of fragments from the highly excited quasiprojectile. In order to make more detailed conclusions about the evolution of the system, a comparison of experimental observables to the results of simulations will be carried out. The simulation will include a model description of the reaction dynamics and a software replica of the FAUST multidetector array (filter routine). For the model description to be considered as adequate we require both ΔA and E^*_{app} to be optimally reproduced for different targets, projectile energies and subsets of data.

The basic assumption on which the simulation is based is the possibility to decompose the collision into two stages. In the early stage of the collision hot quasiprojectiles are created which then deexcite by the statistical decay. To describe the production of excited quasiprojectiles we used the Monte Carlo code of Tassan-Got *et al.* [6]. This code implements a version of the model of deep inelastic transfer suitable for Monte Carlo simulations. For each event, the system evolution is determined by random transfers of nucleons between the projectile and target through an open window between the nuclei. For each transfer, the internal and relative velocities are coupled. Even though the traditional domain of deep inelastic transfer lies at energies below 20 MeV/nucleon, the comparison of the calculated and experimental fragment energy and mass distributions seems to give reasonable agreement up to projectile energies 50 MeV/nucleon when the effect of fragment deexcitation is included [6]. The parameters of the model used in this work are identical to the parameters used in the original work [6]. The number of events generated at a given angular momentum was proportional to the geometrical cross section for a given partial wave. Mean values and widths of the quasiprojectile excitation energy, mass and charge distributions of generated events with intrinsic excitation of the quasiprojectile higher than 35 MeV and $Z_{QP}=12-15$ are given in Table II.

At both projectile energies, the number of neutrons transferred from the target to the projectile increases with the neutron number of the target. A heavier target with a larger neutron number also causes stronger proton flow from the projectile to the target. This behavior is caused by an evolution towards isospin equilibrium between projectile and target and is in qualitative agreement with experimental trends. Mean excitation energies of the simulated quasiprojectiles

TABLE II. Mean values and widths of quasiprojectile excitation energy, mass, and charge distributions simulated using the model of deep inelastic transfer [6]. Only excited quasiprojectiles with $Z_{QP}=12-15$ and intrinsic excitation higher than 35 MeV are included.

E_{proj} (MeV/nucleon)	Target	$\langle A_{QP}\rangle$	$\sigma_{A_{QP}}$	$\langle Z_{QP}\rangle$	$\sigma_{Z_{QP}}$	$\langle E^*_{QP}\rangle$ (MeV)	$\sigma_{E^*_{QP}}$ (MeV)
30	^{112}Sn	28.01	2.36	13.54	1.20	95.5	42.7
	^{124}Sn	28.46	2.15	13.25	1.03	95.1	44.2
50	^{112}Sn	27.91	2.23	13.64	1.19	146.2	78.5
	^{124}Sn	28.19	2.09	13.34	1.04	143.2	79.5

are comparable to the experimental values in Table I and exhibit the same trends for given beam energies and target nuclei. The widths of simulated inclusive excitation energy distributions are larger than the experimental data.

The simulated mean excitation energies of the target are slightly higher than 1 MeV/nucleon for the projectile energy of 30 MeV/nucleon. At 50 MeV/nucleon they reach 1.5 MeV/nucleon. The corresponding temperatures obtained using the well known formula $T=(E^*/\tilde{a})^{1/2}$ are in reasonable agreement with the estimated temperature of the target, when using the asymptotic value of the level density parameter $\tilde{a}=A/9$. At these temperatures, between 3 and 3.5 MeV, the emission of neutrons may be expected to be a dominating deexcitation channel for nuclei with mass and charge close to the target.

In general, the concept of deep inelastic transfer reasonably describes the early stage of the collisions investigated in the present experiment. When combined with a realistic deexcitation model, it may provide a good general description of the reaction mechanism. Since the mean value of excitation energy per nucleon is well above 3 MeV/nucleon for both projectile energies, we simulated the deexcitation of the highly excited quasiprojectile using the statistical model of multifragmentation (SMM) [12]. Macrocanonical partitions of the hot fragments were generated for individual events. For the hot fragments emitted from the quasiprojectile, a multiparticle Coulomb tracking was applied. The final partition of cold fragments was obtained by deexcitation of the hot fragments via Fermi decay and particle emission. The quasiprojectile event sequences generated by the DIT code of Tassan-Got [6] have been used as the input of SMM simulations. The deexcitation of the excited quasitarget was not taken into account as a contributing source of the charged particles at forward angles.

To mimic the experimental selection criteria, we employed restrictions on the kinetic and excitation energy of the simulated quasiprojectiles. Only those events where the quasiprojectiles satisfied the relation

$$\sin\theta_{lim}=\frac{\langle p_f^{QP}\rangle}{\langle p_{f\|}^{lab}\rangle}\approx\sqrt{\frac{E^*_{QP}}{E^{lab}_{kinQP}}}\leqslant 0.6$$

and had intrinsic excitation energy greater than 35 MeV were used as an input to the SMM calculations. This relation rejects the events with fragments emitted outside of the acceptance of our detector setup. The variable $\langle p_f^{QP}\rangle$ is the mean fragment momentum in the quasiprojectile center-of-mass frame, $\langle p_{f\|}^{lab}\rangle$ is the mean value of the component of fragment momentum in the laboratory frame parallel to the beam axis, and E^{lab}_{kinQP} is the kinetic energy of quasiprojectile in the laboratory frame. The initial nuclear density of the fragmenting quasiprojectile was equal to the equilibrium nuclear density. The SMM events with all fragments having $Z_f\leqslant 5$ were filtered by the FAUST software replica, which simulates the geometrical coverage of FAUST and the energy thresholds of the telescopes for a given fragment mass and charge. The results of the simulation are shown in Figs. 4 and 5. The simulated distributions of the mass change for fully isotopi-

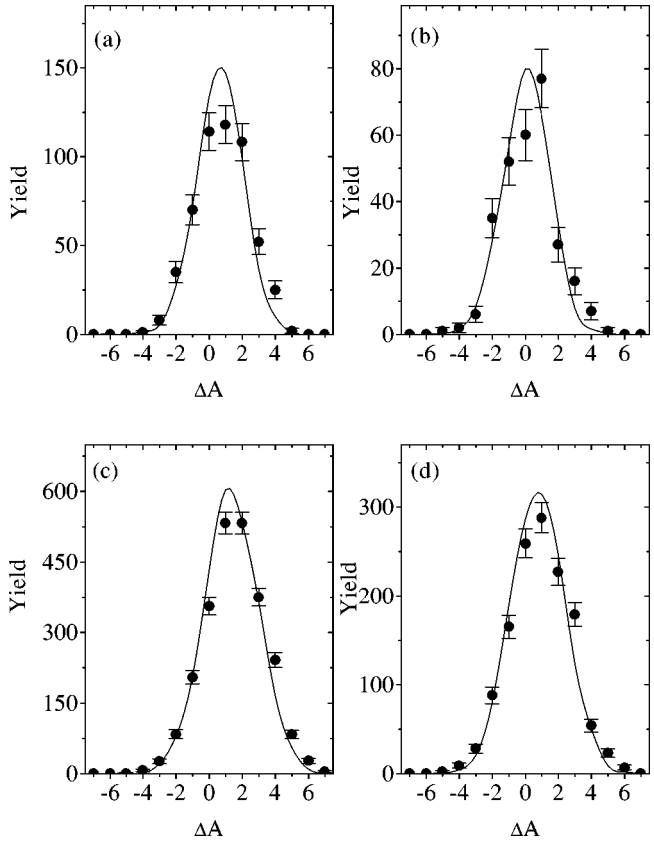

FIG. 4. Experimental (solid circles) and simulated (solid lines) mass change distributions for the fully isotopically resolved quasiprojectiles with $Z_{tot}=14$, (a) ^{28}Si(30 MeV/nucleon)+^{112}Sn, (b) ^{28}Si(30 MeV/nucleon)+^{124}Sn, (c) ^{28}Si(50 MeV/nucleon)+^{112}Sn, (d) ^{28}Si(50 MeV/nucleon)+^{124}Sn. For details of simulation see text.

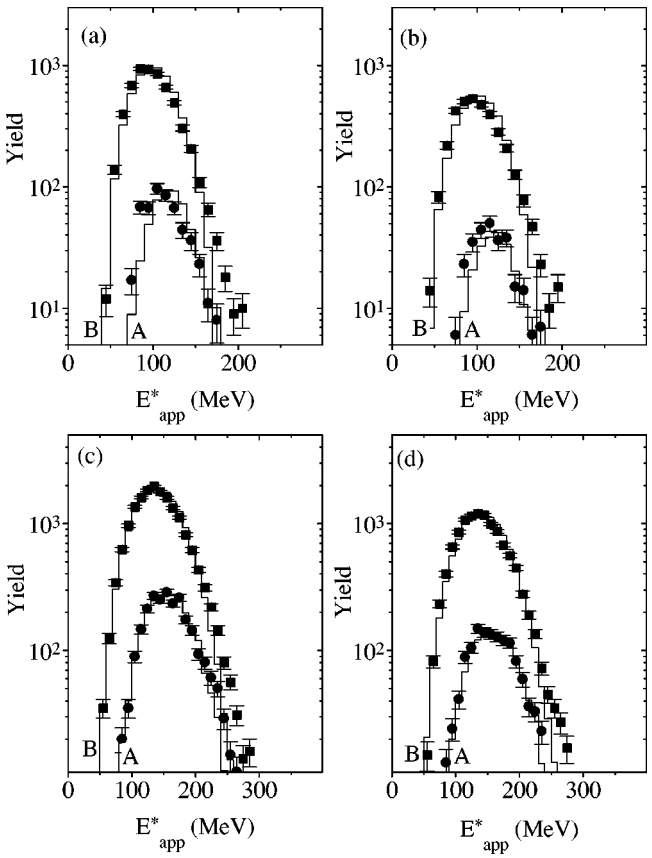

FIG. 5. Distributions of the reconstructed apparent excitation energies of the quasiprojectiles. Symbols mean experimental distributions of the set of fully isotopically resolved quasiprojectiles with $Z_{tot}=14$ (solid circles) and $Z_{tot}=12-15$ (solid squares). Solid histograms labeled as A and B mean simulated distributions for $Z_{tot}=14$ and $Z_{tot}=12-15$, (a) ^{28}Si(30 MeV/nucleon)+^{112}Sn, (b) ^{28}Si(30 MeV/nucleon)+^{124}Sn, (c) ^{28}Si(50 MeV/nucleon)+^{112}Sn, (d) ^{28}Si(50 MeV/nucleon)+^{124}Sn. For details of simulations see text.

cally resolved events with $Z_{tot}=14$ (solid lines) are plotted in Fig. 4 (solid circles represent experimental data) normalized to the number of experimental events with $Z_{tot}=14$. The agreement of the experimental and simulated distributions of the mass change is quite good. In Fig. 5 the simulated distributions of the apparent quasiprojectile excitation energy are shown for both $Z_{tot}=14$ and $Z_{tot}=12-15$ (solid histograms labeled as A and B, respectively) along with the experimental data (solid circles and squares, respectively). The simulated data have been normalized to the sum of experimental events with $Z_{tot}=12-15$. The agreement of the simulated and experimental apparent quasiprojectile excitation energy distributions with both $Z_{tot}=12-15$ and $Z_{tot}=14$ is quite good. The onset of multifragmentation into channels with $Z_f \leqslant 5$ in the low-energy part is described with good precision for both sets of data $Z_{tot}=12-15$ and $Z_{tot}=14$.

The mean values of the mass and charge of the quasiprojectiles with $Z_{tot}=12-15$ obtained from the simulation are comparable with the values, obtained from experimental mass and charge distributions (see Table III). The simulation is able to reproduce the trends of the nucleon exchange also for the broader set of contributing events which are not taken into account in the analysis of ΔA.

The overall agreement in Figs. 4 and 5 and Table III shows that a combination of the concepts of deep inelastic transfer and statistical multifragmentation satisfactorily describes the data. The influence of the target neutron number and beam energy is reproduced correctly not only on average, but even for different subsets of data. Using a backtracing procedure we estimated the range of contributing angular momenta in the simulated data. The mean values are 186 and 203 $\hbar$ for ^{112}Sn and ^{124}Sn targets at projectile energy 30 MeV/nucleon and 243 and 263 $\hbar$ for 50 MeV/nucleon, respectively. When converting angular momentum to impact parameter, the mean values are 5.5 and 5.6 fm for ^{112}Sn and ^{124}Sn targets at projectile energy 30 MeV/nucleon and 5.9 and 6.0 fm at the higher projectile energy. Estimated mean values are well below the contact (grazing) configuration for both reactions, which can be roughly estimated with $R_{12}=r_0(A_P^{1/3}+A_T^{1/3})+1$ fm. When taking $r_0=1.12$ fm, corresponding to half-density radii, the R_{12} equals 9.8 and 10.0 fm for ^{112}Sn and ^{124}Sn, respectively. The estimated range of contributing impact parameters corresponds to peripheral collisions.

Using the backtracing procedure, we estimated the mean multiplicity of neutrons emitted from the quasiprojectile. Mean values of the multiplicity of emitted neutrons are 0.9 and 1.2 for ^{112}Sn and ^{124}Sn targets at projectile energy 30 MeV/nucleon and 1.4 and 1.7 for ^{112}Sn and ^{124}Sn targets at projectile energy 50 MeV/nucleon, respectively. The mean values of the multiplicity of emitted neutrons increase with increasing projectile energy while the effect of target neutron excess is relatively weak. Using the estimated multiplicities of emitted neutrons, we determined the mean values of the N/Z ratio of the excited quasiprojectiles to be 1.04 and 1.12 for ^{112}Sn and ^{124}Sn targets at projectile energy 30 MeV/

TABLE III. Mean values of the mass and charge of the reconstructed quasiprojectiles with $Z_{tot}=12-15$. Experimental values are compared to the results of simulation. For details of simulation see text.

E_{proj} (MeV/nucleon)	Target	$\langle Z_{QP}\rangle$ Exp.	$\langle Z_{QP}\rangle$ Sim.	$\langle A_{QP}\rangle$ Exp.	$\langle A_{QP}\rangle$ Sim.
30	^{112}Sn	12.55±0.26	12.51±0.11	24.36±0.56	24.65±0.25
	^{124}Sn	12.50±0.33	12.39±0.11	25.00±0.71	25.15±0.25
50	^{112}Sn	12.74±0.17	12.72±0.10	24.33±0.34	24.68±0.24
	^{124}Sn	12.67±0.19	12.61±0.10	24.83±0.39	24.96±0.24

nucleon and 1.03 and 1.11 for ^{112}Sn and ^{124}Sn targets at projectile energy 50 MeV/nucleon, respectively. The mean values of the N/Z ratio for the different projectile energies only slightly differ. The effect of target isospin is significant and is similar at both projectile energies. The estimated values of the N/Z ratio of the hot quasiprojectile are consistent with the simulated mean values of the mass and charge of excited quasiprojectiles given in Table II.

Even if the projectile energies are relatively high, the data do not appear to be strongly influenced by preequilibrium emission. For the protons, which are primary candidates for preequilibrium emission among particles observed in the present experiment, we determined their momenta in the quasiprojectile frame and constructed two-dimensional plots of the momentum component parallel to the quasiprojectile direction versus the momentum of quasiprojectile in the lab frame. In the experimental distributions for the ^{112}Sn target, two different sources could be identified, a stronger one in the forward hemisphere and a weaker one in the backward hemisphere of the quasiprojectile. The experimental distributions for the ^{124}Sn target consisted only of the particles in forward hemisphere, which was fully compatible with the forward source in the previous case. This feature is unique for protons and does not exist in the case of heavier fragments. According to the conclusions of Ref. [1], the protons in forward hemisphere of the quasiprojectile are emitted from the quasiprojectile during multifragmentation and are later shifted forward by the Coulomb field of the target because of the high charge to mass ratio compared to other fragments. The systematics of Coulomb shifts observed in our data tracks well with the results of Ref. [1]. Thus, in the case of ^{112}Sn target, the protons in the backward hemisphere can be attributed to preequilibrium emission. The absence of such a source in the case of ^{124}Sn target can be explained by the emission of preequilibrium neutrons from this more neutron rich system which are not detected in our experiment. From the event rate in this component, we estimated the multiplicity of preequilibrium protons accompanying multifragmentation of the fully isotopically resolved quasiprojectiles with $Z_{\rm tot}=12-15$ as 0.2 ± 0.1 for the projectile energy 30 MeV/nucleon and 0.3 ± 0.1 for the projectile energy 50 MeV/nucleon. Such rates are quite moderate and the physical picture used by the simulation remains valid.

To summarize this section, we presented a unique set of isotopically resolved projectile multifragmentation data and determined the dominant mechanism of nucleon exchange, but not without using model assumptions about deexcitation of the excited quasiprojectile. In the next section we will discuss the deexcitation of the quasiprojectile in detail.

QUASIPROJECTILE MULTIFRAGMENTATION

In order to obtain a fully isotopically resolved event with $Z_f \leqslant 5$, the quasiprojectiles with $Z_{\rm tot}=12-15$ have to disintegrate into at least three charged particles. As already shown in Fig. 5, the simulation is capable of correctly describing the onset of this fragmentation mode and the overall quasiprojectile excitation energy distribution for the quasiprojectiles with the charge close to the charge of the projectile. The

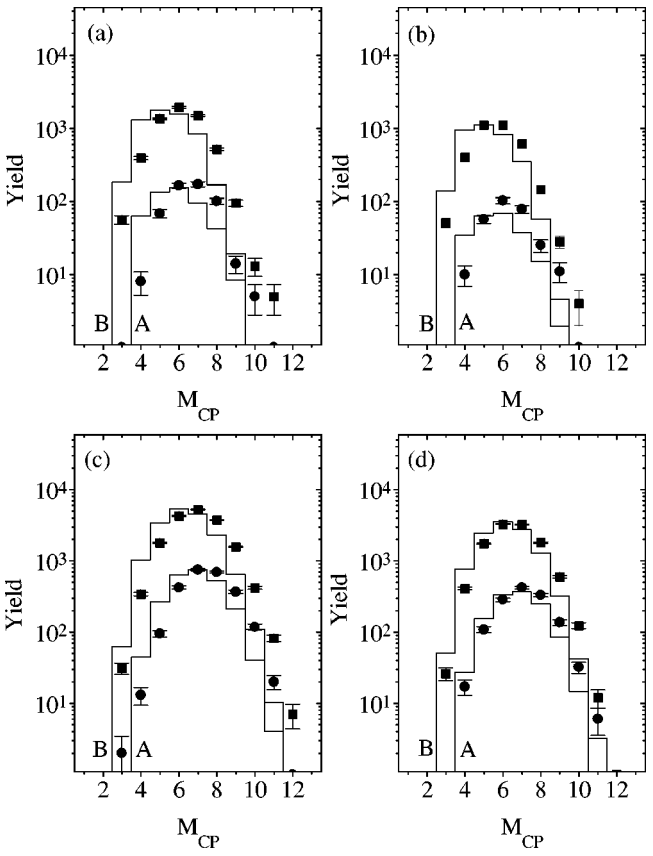

FIG. 6. Experimental multiplicity distributions of charged particles emitted from the fully isotopically resolved quasiprojectiles with $Z_{\rm tot}=14$ (solid circles) and $Z_{\rm tot}=12-15$ (solid squares) and the results of simulation for the same sets of data (histograms labeled as A and B). (a) ^{28}Si(30 MeV/nucleon)+^{112}Sn, (b) ^{28}Si(30 MeV/nucleon)+^{124}Sn, (c) ^{28}Si(50 MeV/nucleon)+^{112}Sn, (d) ^{28}Si(50 MeV/nucleon)+^{124}Sn. For details of simulations see text.

experimental distributions of charged particle multiplicity are presented in Fig. 6 for isotopically resolved data with $Z_{\rm tot}=14$ (solid circles) and $Z_{\rm tot}=12-15$ (solid squares). The simulations are presented as histograms labeled as A ($Z_{\rm tot}=14$) and B ($Z_{\rm tot}=12-15$). The calculations are normalized to the experimental data by the sum of isotopically resolved quasiprojectiles with $Z_{\rm tot}=12-15$. The simulated data in Fig. 6 show reasonable overall agreement with the results of experiment. The simulated distributions are shifted to somewhat lower values of multiplicity. Table IV presents the mean values of the fragment multiplicity and fragment charge for both experiment and simulation. The simulated mean fragment multiplicities are smaller than the experimental ones. The difference ranges from 0.2 to 0.6 and is slightly larger in the case of ^{112}Sn. The simulated mean values (see Table IV) of the fragment charge are larger than the experimental ones, thus counterbalancing a smaller fragment number. The fragment charge yields (see Fig. 7) show analogous yields of fragments with $Z_f=1$, the simulated yields of fragments with $Z_f=2$ are smaller than the experimental ones by about 10% and the simulated yields of heavier fragments are higher than the experimental ones. Higher experimental yield

TABLE IV. Mean values of the multiplicity, charge, and N/Z ratio of the charged fragments, emitted in events where the quasiprojectiles with $Z_{tot}=12-15$ were fully isotopically resolved. Experimental values are compared to the results of simulation. For details of simulation see text.

E_{proj} (MeV/nucleon)	Target	$\langle M_{CP}\rangle$ Exp.	$\langle M_{CP}\rangle$ Sim.	$\langle Z_f\rangle$ Exp.	$\langle Z_f\rangle$ Sim.	$\langle N/Z\rangle$ Exp.	$\langle N/Z\rangle$ Sim.
30	^{112}Sn	5.95±0.11	5.37±0.04	2.11±0.02	2.33±0.01	0.95±0.02	0.97±0.01
	^{124}Sn	5.63±0.14	5.14±0.04	2.22±0.02	2.41±0.01	1.01±0.02	1.03±0.01
50	^{112}Sn	6.74±0.08	6.33±0.04	1.89±0.01	2.01±0.01	0.91±0.01	0.94±0.01
	^{124}Sn	6.43±0.09	6.21±0.04	1.97±0.01	2.03±0.01	0.96±0.01	0.98±0.01

of α particles may be influenced by the existence of preformed α clusters in the projectile nucleus ^{28}Si. The data presented applies to isotopically resolved events with $Z_{tot}=12-15$. Similar distributions for subsets of data with $Z_{tot}=14$ give identical results.

Additional understanding of quasiprojectile deexcitation may be obtained from the study of isospin degrees of freedom. The overall values of the N/Z of the quasiprojectile are similar for the experiment and the simulations (see Table IV). The results of simulation are slightly higher in all cases but the difference is within the statistical errors. The situation is significantly different when investigating the fragments of different charges independently. In Fig. 8, we present average N/Z ratios for fragments with different charges. The data presented applies to isotopically resolved events with $Z_{tot}=12-15$. The results for subsets of data with $Z_{tot}=14$ are practically identical. Experimental N/Z ratios show an excess of neutron rich fragments with $Z_f\geqslant 3$ relative to the simulation, counterbalanced by stronger dominance of protons among the fragments with $Z_f=1$. This may point out

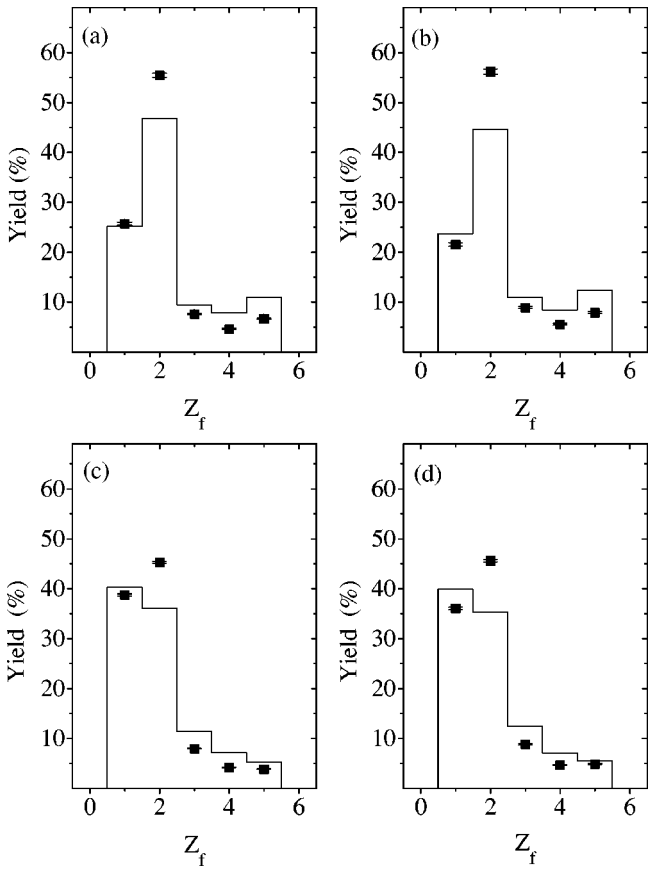

FIG. 7. Experimental (solid squares) and simulated (solid histograms) charge distributions of fragments emitted from the fully isotopically resolved quasiprojectiles with $Z_{tot}=12-15$, (a) ^{28}Si(30 MeV/nucleon)+^{112}Sn, (b) ^{28}Si(30 MeV/nucleon)+^{124}Sn, (c) ^{28}Si(50 MeV/nucleon)+^{112}Sn, (d) ^{28}Si(50 MeV/nucleon)+^{124}Sn. For details of simulations see text.

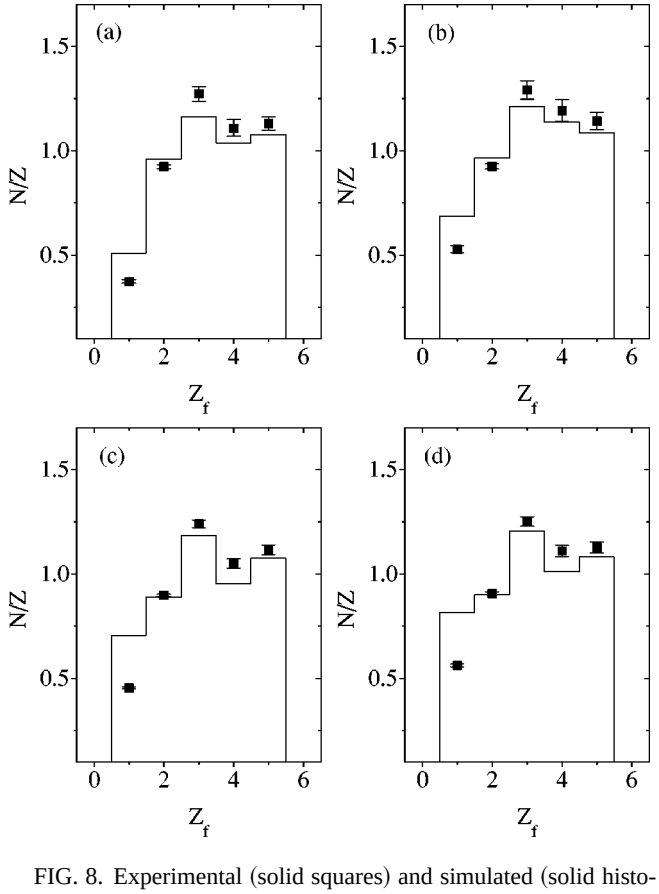

FIG. 8. Experimental (solid squares) and simulated (solid histograms) dependences of mean fragment N/Z ratio on the charge of fragments emitted from the fully isotopically resolved quasiprojectiles with $Z_{tot}=12-15$, (a) ^{28}Si(30 MeV/nucleon)+^{112}Sn, (b) ^{28}Si(30 MeV/nucleon)+^{124}Sn, (c) ^{28}Si(50 MeV/nucleon)+^{112}Sn, (d) ^{28}Si(50 MeV/nucleon)+^{124}Sn. For details of simulations see text.

a higher decay probability of the excited neutron deficient quasiprojectiles or hot fragments for the channels with emission of stable charged particles like protons and α particles. Alternatively, the relative excess of protons may be caused by preequilibrium emission, especially in the case of less neutron rich target ^{112}Sn. When comparing the sensitivity of experimental N/Z ratios to the neutron content of the target at given projectile energy, the N/Z ratios of fragments with $Z_f=1$ and $Z_f=4$ show the highest sensitivity. This trend was reported in our previous study where a broader set of data was presented [8].

For the case of ^{8}Li, which could be influenced by an admixture of the two α-particle decay of short-lived ^{8}Be, we compared the experimental and simulated values of the isotopic ratio Y(^{8}Li)/Y(^{7}Li) for different bins of the isospin of the quasiprojectile. Detection of ^{8}Be was *a priori* excluded in the simulation. We found no significant deviations between experimental data and simulation, which allows us to conclude that the admixture of ^{8}Be in the yield of ^{8}Li does not dramatically influence the results of our analysis.

In summary, the overall description of the experimental data on charged particle multiplicity, charge distributions, and isotopic ratios may be considered as reasonable in general. The remaining minor inconsistencies may be attributed to the limitations in the model description of quasiprojectile deexcitation and/or to the influence of preequilibrium emission. These inconsistencies, however, do not influence conclusions concerning the mechanism of nucleon exchange given in previous section.

SUMMARY

Using the FAUST detector array we obtained a set of fully isotopically resolved projectile multifragmentation events ($Z_f \leqslant 5$) from the reactions ^{28}Si+^{112,124}Sn at projectile energies 30 and 50 MeV/nucleon. We have been able to reconstruct the mass, charge and dynamic observables of the excited quasiprojectile and to study the nucleon exchange between projectile and target. The reconstructed velocity distributions of the emitting source have been fitted using one Gaussian source. Thus admixtures from a midvelocity source can be excluded. At a given projectile energy, we observed an influence of the target isospin on the mass change of the reconstructed quasiprojectiles that have the charge of the beam ($Z_{\mathrm{tot}}=14$). However, we observed no significant influence of the target isospin on the apparent excitation energy distribution. Reactions with a heavier target isotope result in lower average mass change. This may be seen as evidence for partial equilibration of isospin in the early stage of the reaction. In the reactions with the same target the mass change increases with increasing projectile energy. This corresponds to a shift in the distributions of apparent quasiprojectile excitation energies toward higher values. The influence of the target isospin and of the projectile energy on the neutron content of the reconstructed quasiprojectiles can be explained by a two stage model consisting of nucleon exchange in the early stage of collision followed by deexcitation of the quasiprojectile.

The experimental observables for different subsets of data were reproduced using a simulation using the concept of deep inelastic transfer in the early stage followed by quasiprojectile multifragmentation and sequential decay of the hot fragments. The deexcitation of the excited quasitarget and the preequilibrium emission were not taken into account in our simulation. Distributions of the mass change and apparent excitation energy of reconstructed quasiprojectiles have been reproduced with good overall agreement. The charged fragment multiplicities, charge distributions and N/Z ratios for different fragment charges imply lower experimental survival probability of neutron deficient fragments towards decay into stable light charged particles than predicted by the simulation. We observed a maximum of the sensitivity of the N/Z ratios to the target isospin for the fragment charges $Z_f=1$ and $Z_f=4$. The contributing range of impact parameters was estimated by backtracing the simulated data ($b=5-7$ fm) indicating that the collisions may be considered as nearly peripheral. Observables related to target multifragmentation and preequilibrium emission imply that neither of the processes causes significant distortion of the physical picture used in the simulation. The backtracing of simulated data allowed an estimation of the multiplicity of neutrons emitted from the quasiprojectile in the deexcitation stage. The estimated neutron multiplicities allowed further determination of the corresponding level of isospin equilibration between projectile and target during the nucleon exchange stage, which strongly depends on target isospin. The present work shows that deep inelastic transfer is the dominant production mechanism of highly excited quasiprojectiles in peripheral collisions in the Fermi energy domain and that such collisions are suitable for detailed studies of thermal multifragmentation.

ACKNOWLEDGMENTS

The authors wish to thank the Cyclotron Institute staff for the excellent beam quality. This work was supported in part by the NSF through Grant No. PHY-9457376, the Robert A. Welch Foundation through Grant No. A-1266, and the U.S. Department of Energy through Grant No. DE-FG03-93ER40773. M.V. was partially supported through Grant No. VEGA-2/5121/98.

[1] R. J. Charity *et al.*, Phys. Rev. C **52**, 3126 (1995).

[2] R. T. de Souza, J. R. Huizenga, and W. U. Schröder, Phys. Rev. C **37**, 1901 (1988); R. T. de Souza, W. U. Schröder, J. R. Huizenga, J. Tõke, S. S. Datta, and J. L. Wile, *ibid.* **39**, 114 (1989).

[3] R. T. de Souza, W. U. Schröder, J. R. Huizenga, R. Planeta, K. Kwiatkowski, V. E. Viola, and H. Breuer, Phys. Rev. C **37**, 1783 (1988).

[4] R. Planeta *et al.*, Phys. Rev. C **38**, 195 (1988).
[5] J. Randrup, Nucl. Phys. **A307**, 319 (1978); **A327**, 490 (1979); **A383**, 468 (1982).
[6] L. Tassan-Got and C. Stéfan, Nucl. Phys. **A524**, 121 (1991).
[7] G. J. Kunde *et al.*, Phys. Rev. Lett. **77**, 2897 (1996).
[8] R. Laforest, E. Ramakrishnan, D. J. Rowland, A. Ruangma, E. M. Winchester, E. Martin, and S. J. Yennello, Phys. Rev. C **59**, 2567 (1999).
[9] F. Gimeno-Nogues *et al.*, Nucl. Instrum. Methods Phys. Res. A **399**, 94 (1997).
[10] R. Laforest, E. Ramakrishnan, D. J. Rowland, R. Delafield, S. Guzman, S. Ferro, S. Vasal, E. Winchester, and S. J. Yennello, Nucl. Instrum. Methods Phys. Res. A **404**, 470 (1998).
[11] H. Feldmeier, Rep. Prog. Phys. **50**, 915 (1987).
[12] J. P. Bondorf, A. S. Botvina, A. S. Iljinov, I. N. Mishustin, and K. Sneppen, Phys. Rep. **257**, 133 (1995).